Constitutive CD40 Signaling in B Cells Selectively Activates the Noncanonical NF-κB Pathway and Promotes Lymphomagenesis

Constitutive CD40 signaling in B cells selectively activates the noncanonical NF-κB pathway and promotes lymphomagenesis

Cornelia Hömig-Hölzel,[1] Caroline Hojer,[1] Julia Rastelli,[1] Stefano Casola,[2] Lothar J. Strobl,[1] Werner Müller,[3] Leticia Quintanilla-Martinez,[4] Andreas Gewies,[5] Jürgen Ruland,[5] Klaus Rajewsky,[2] and Ursula Zimber-Strobl[1]

[1]Institute of Clinical Molecular Biology and Tumor Genetics, Helmholtz Center Munich, German Research Center for Environment and Health, D-81377 Munich, Germany
[2]Immune Disease Institute, Harvard Medical School, Boston, MA 02115
[3]The Department of Experimental Immunology, Helmholtz Center for Infectious Research, D-38124 Braunschweig, Germany
[4]Institute of Pathology, Helmholtz Center Munich, German Research Center for Environment and Health, D-85764 Neuherberg, Germany
[5]III Med. Department, Technical University of Munich, Klinikum rechts der Isar, D-81675 Munich, Germany

CD40, a member of the tumor necrosis factor (TNF) receptor family, plays an essential role in T cell–dependent immune responses. Because CD40 is widely expressed on the surface of tumor cells in various B cell malignancies, deregulated CD40 signaling has been suggested to contribute to lymphomagenesis. In this study, we show that B cell–specific expression of a constitutively active CD40 receptor, in the form of a latent membrane protein 1 (LMP1)/CD40 chimeric protein, promoted an increase in the number of follicular and marginal zone B cells in secondary lymphoid organs in transgenic mice. The B cells displayed an activated phenotype, prolonged survival and increased proliferation, but were significantly impaired in T cell–dependent immune responses. Constitutive CD40 signaling in B cells induced selective and constitutive activation of the noncanonical NF-κB pathway and the mitogen-activated protein kinases Jnk and extracellular signal–regulated kinase. LMP1/CD40-expressing mice older than 12 mo developed B cell lymphomas of mono- or oligoclonal origin at high incidence, thus showing that the interplay of the signaling pathways induced by constitutive CD40 signaling is sufficient to initiate a tumorigenic process, ultimately leading to the development of B cell lymphomas.

The Journal of Experimental Medicine

CORRESPONDENCE
Ursula Zimber-Strobl:
strobl@helmholtz-muenchen.de

Abbreviations used: Erk, extracellular signal–regulated kinase; ES, embryonic stem; GC, germinal center; HE, hematoxylin and eosin; LMP, latent membrane protein; MAPK, mitogen-activated protein kinase; TD, T cell dependent.

CD40, which is a member of the TNF receptor superfamily, is expressed on virtually all mature B lymphocytes and on most of their neoplastic counterparts. Upon interaction with CD40 ligand (CD40L), which is predominantly expressed on activated $CD4^+$ T cells, CD40 promotes B cell activation, proliferation, survival, and up-regulation of surface molecules involved in antigen presentation (1). The finding that patients suffering from "X-linked hyper-IgM syndrome" have a defect in expression of CD40L was instrumental in the discovery that CD40–CD40L interactions play a crucial role in T cell–dependent (TD) immune response (2, 3), contributing to germinal center (GC) formation, memory B cell development, Ig isotype switching, and affinity maturation (4, 5).

The cytoplasmic tail of CD40, which lacks intrinsic catalytic activity, delivers signals to the cells by recruitment of TNF receptor–associated factors 1, 2, 3, 5, and 6. Interaction with its ligand leads to clustering of CD40 in lipid rafts and, finally, to the recruitment of TNF receptor–associated factor molecules (6, 7). These events

C. Hömig-Hölzel and C. Hojer contributed equally to this paper.

S. Casola's present address is IFOM-The Foundation for Cancer Research Institute of Molecular Oncology, 20139 Milan, Italy.

C. Hömig-Hölzel's present address is Division of Molecular Genetics, Netherlands Cancer Institute, Amsterdam, Netherlands.

J. Rastelli's present address is Whitehead Institute for Biomedical Research, Cambridge, MA 02142.

The online version of this article contains supplemental material.

The Rockefeller University Press $30.00
J. Exp. Med. Vol. 205 No. 6 1317-1329 www.jem.org/cgi/doi/10.1084/jem.20080238

initiate downstream signaling, resulting in activation of phosphoinositide 3 kinase, phospholipase Cγ, mitogen-activated protein kinases (MAPKs), and NF-κB (1, 6). Additionally, the Janus family kinase 3 (JAK3), which is associated with the cytoplasmic tail of CD40, undergoes phosphorylation, resulting in the activation of the signal transducer and activator of transcription 3 (8).

The following three subfamilies of structurally related MAPKs are activated by CD40: extracellular signal-regulated kinase 1 (Erk1) and Erk2, the c-jun kinases Jnk1 and Jnk2, and the kinase p38/MAPK (9–11). MAPKs are serine/threonine protein kinases, which are activated by dual phosphorylation on a specific tyrosine and threonine residue, respectively. After activation, MAPKs phosphorylate nuclear substrates such as the transcription factors c-Jun, Elk-1, Egr-1, and Atf-2, which in turn bind to specific DNA sequences and thus modulate transcription (1, 6).

CD40 signaling activates both the canonical and the noncanonical NF-κB signaling pathways (12, 13). In mammals, the NF-κB family consists of five genes coding for NF-κB1 (p105/p50), NF-κB2 (p100/p52), RelA (p65), RelB, and c-Rel (14). In unstimulated cells, the DNA-binding activity of NF-κB dimers is inhibited through the interaction with proteins of the inhibitor of the NF-κB (IκB) family. The activation of the canonical NF-κB signaling pathway largely depends on ubiquitin-dependent degradation of small IκB proteins, leading to the nuclear translocation of NF-κB heterodimers p50/p65 and p50/c-Rel. The liberated heterodimers are capable of binding DNA, and thereby activating gene expression. The noncanonical pathway depends on proteolytic cleavage of the precursor p100, liberating mainly p52/RelB heterodimers for nuclear translocation. Thus, canonical and noncanonical NF-κB signaling pathways induce the formation and nuclear translocation of distinct NF-κB heterodimers that activate distinct target genes (15–17).

Whereas CD40 plays a decisive role in TD immune responses, aberrant CD40 signaling is suspected to play a critical role in the oncogenic processes of various cell types, including B cells (18). CD40 is widely expressed in B cell lymphomas and in selected carcinomas. Additionally, aberrant CD40L expression, which may lead to constitutive CD40 engagement, has been observed in several malignancies, including chronic lymphocytic leukemia, mantle cell lymphoma, follicular lymphoma, Burkitt's lymphoma, and breast cancer (19–22). Thus, a contribution of this receptor to tumor pathogenesis has been suggested.

However, it is unclear whether aberrant CD40 signaling is sufficient to drive lymphomagenesis or whether it is only involved in the maintenance of established malignancies. Adequate experimental systems to explore this question are still missing. To study the biological and potential pathological effects of a constitutive CD40 activation, we generated knock-in mice expressing in a conditional manner a chimeric protein consisting of the transmembrane domain of the Epstein-Barr viral latent membrane protein 1 (LMP1) and the intracellular signaling domain of CD40 (LMP1/CD40). This chimeric protein is able to deliver a ligand-independent constitutive CD40 signal by promoting self-aggregation in the plasma membrane (23, 24). Constitutive CD40 signaling in B cells led to a strong accumulation of follicular and marginal zone B cells in secondary lymphoid organs, accompanied by a significant enlargement of follicles. These B cells displayed an activated phenotype, but failed to form GCs in response to immunization with TD antigens. Ultimately, LMP1/CD40-expressing mice developed mono- or oligoclonal B cell lymphomas at high incidence, demonstrating that deregulated CD40 signaling is sufficient to initiate B cell transformation.

RESULTS

Generation of transgenic mice expressing a conditional LMP1/CD40 transgene

To study constitutive CD40 signaling in vivo, mice expressing a fusion protein comprising the signaling domain of the human CD40 and the transmembrane domain of LMP1 (LMP1/CD40) were generated. It had been shown earlier that human *CD40* can rescue the phenotype of *CD40*-deficient mice, indicating that the receptors of both species are functionally equivalent (25). A copy of the *LMP1/CD40* chimeric gene was inserted into the murine *rosa26* genomic locus of BALB/c-derived embryonic stem (ES) cells by homologous recombination (Fig. 1 A). To restrict expression of *LMP1/CD40* in a cell type– and stage-specific manner, we inserted a loxP-flanked transcription and translation termination sequence (stop cassette) upstream of the *LMP1/CD40* coding sequence. After Cre-mediated excision of the stop-cassette, the *LMP1/CD40* transgene is placed under the control of the ubiquitously active *rosa26* promoter. Correctly targeted ES cell clones were identified by Southern blot analysis and used to establish the LMP1/CD40^{flSTOP} mouse strain.

The LMP1/CD40^{flSTOP} mice were crossed to CD19-Cre and CD21-Cre mice to activate expression of the chimeric protein from earlier (pro–/pre–) or later (mature) stages of B cell development, respectively (26, 27). Because offspring of both crosses revealed the same immunological phenotype, results are presented for mice obtained from LMP1/CD40^{flSTOP};CD19-Cre crosses only. In all biochemical experiments, only LMP1/CD40^{flSTOP};CD19-Cre were analyzed. For simplicity, mice carrying one LMP1/CD40 knock-in allele and one CD19-Cre allele will be referred to as LMP1/CD40 mice. As controls, either LMP1/CD40^{flSTOP} or CD19-Cre mice were used. These control strains had an identical phenotype. In LMP1/CD40 mice, deletion of the stop cassette could be detected in about half of BM and in almost all splenic B cells (Fig. 1 B). This is consistent with previous reports showing a gradual increase in Cre-mediated recombination in CD19-Cre mice as B cells proceed through their differentiation (27). Expression of the LMP1/CD40 protein in splenic cells after removal of the stop cassette was analyzed by Western blot analysis (Fig. 1 C). LMP1/CD40 protein expression was detected in splenocytes isolated from LMP1/CD40 mice, but not in control mice (Fig. 1 C), indicating that LMP1/CD40 is expressed after Cre-mediated recombination and confirming

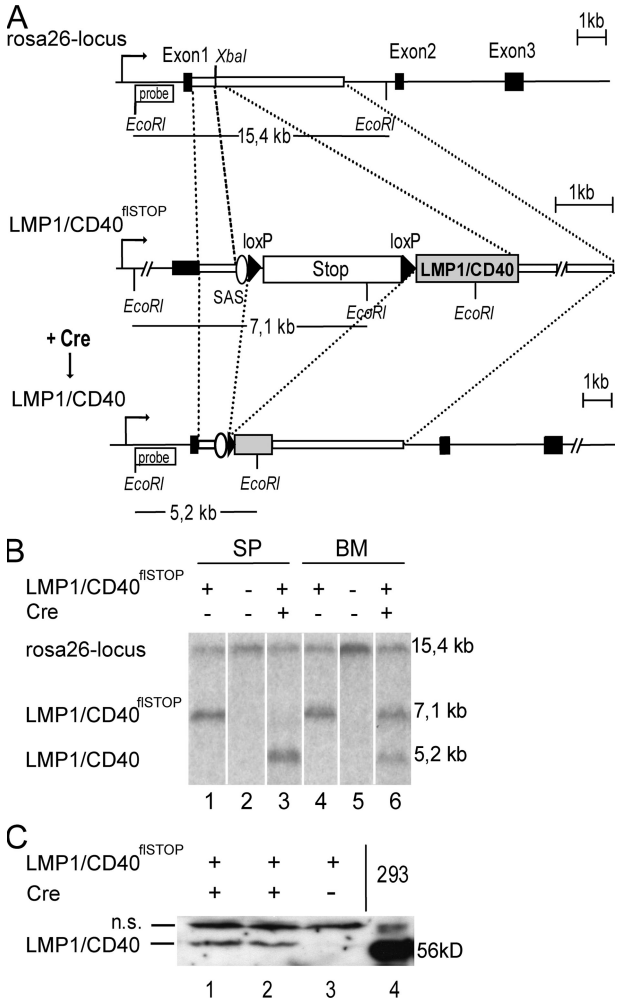

Figure 1. Generation of transgenic mice conditionally expressing LMP1/CD40. (A) Targeting strategy for the insertion of a conditional *LMP1/CD40* allele *(LMP1/CD40^{flSTOP})* into the murine *rosa26*-locus. Cre-mediated recombination leads to deletion of the stop cassette and expression of *LMP1/CD40* under transcriptional control of the endogenous *rosa26*-promoter. The scheme of the targeting construct shows the EcoRI recognition sites and the location of the probe. The expected fragments after EcoRI digestion and hybridization with the labeled probe are indicated by the thin lines. SAS, splice acceptor site; STOP, Stop cassette, XbaI, site of insertion. (B) Southern blot analysis of EcoRI-digested genomic DNA showing the deletion efficiency of the stop cassette in B cells of the spleen (SP; lane 3) and the BM (lane 6) of LMP1/CD40 mice. DNA from B cells of control mice (lanes 2 and 5) and mice heterozygous for *LMP1/CD40^{flSTOP}* (lane 1 and 4) was included. B cells were purified by using magnetic beads against CD19. After deletion of the stop cassette, the rosa26 probe detects a 5.2-kb fragment (LMP1/CD40). The 15- and 7.1-kb fragments represent the wild-type *rosa26* allele (*rosa26* locus) and the targeted allele (*LMP1/CD40^{flSTOP}*), respectively. The deletion efficiency was ~50% in the BM and almost complete in the spleen. (C) LMP1/CD40 protein expression. Western blots were prepared from spleen lysates of LMP1/CD40;CD19-Cre (lanes 1 and 2) and control mice (lane 3). As control, protein lysates of 293 cells transiently transfected with a LMP1/CD40 expression vector were included in the analysis (lane 4). The 56-kD LMP1/CD40 chimeric protein was detected by an anti–human CD40 antibody. ns, nonspecific band.

the tight control exerted by the stop cassette on transgene expression. To study whether the LMP1/CD40 fusion protein can substitute for CD40 in B cells, we tested its ability to promote Ig class switch recombination. We isolated splenic lymphocytes from LMP1/CD40 mice and stimulated them ex vivo with anti-CD40 agonistic antibody (α-CD40), IL-4, or α-CD40 plus IL-4. After 5 d, a distinct fraction of IgG1 class-switched cells could be detected in cultures of LMP1/CD40-expressing B cells upon stimulation with IL-4 only, whereas in the controls, IgG1$^+$ cells appeared only after co-stimulation with α-CD40 and IL-4 (Fig. S1, available at http://www.jem.org/cgi/content/full/jem.20080238/DC1). These data indicate that LMP1/CD40 induces Ig class switch recombination in the presence of IL-4, and thus constitutive CD40 signaling in murine B cells.

Increase of B and T cell numbers in LMP1/CD40 mice

Conditional expression of LMP1/CD40 in B cells resulted in a splenomegaly in 8–16-wk-old mice (Fig. 2 A). The splenic weight of LMP1/CD40-expressing mice was, on average, increased by 3.5-fold compared with that of control mice (unpublished data). The splenomegaly was largely dependent on the increased number of B cells and, to a lesser degree, T cells. On average, eight times more B cells and three times more T cells were recovered from spleens of LMP1/CD40 mice compared with age-matched controls (Fig. 2 B). Immunohistochemical analysis of the spleen revealed that the overall follicular structure with the respective B and T cell zones, as well as the marginal zone, was retained (Fig. 2 C). The size of the follicles, however, was significantly increased, with a larger expansion of the B cell compared with the T cell zone.

In LNs of LMP1/CD40 mice, absolute numbers of B cells were, on average, increased by fourfold compared with those of control mice, whereas absolute B cell numbers in the BM of mutant mice were unaffected (Fig. 2 D).

LMP1/CD40–expressing B cells display an activated phenotype, but fail to form GCs

To determine the distribution of B cell subsets in LMP1/CD40 mice, cells from BM, spleen, and inguinal LNs of experimental and control animals were stained for various surface markers and analyzed by flow cytometry. In LMP1/CD40 mice, the percentage of IgM$^+$IgD$^+$ B cells was significantly increased in spleen and LN (Fig. 3 A). In the spleen, the percentage of marginal zone B cells was increased and numbers of CD21$^+$CD23$^+$ follicular and CD21^{high}CD23^{low} marginal zone B cells were, respectively, 8 and 12 times higher than those of controls (Fig. 3, B and C). In the BM, the percentages of pro–, pre–, immature, and mature B cells were comparable in mutant and control mice (unpublished data). Flow cytometric analysis of the expression level of various activation and adhesion molecules revealed an increase in surface expression of CD95, ICAM-1, MHC class II, CD80, and CD86 in B cells isolated from the spleen and LN of LMP1/CD40 mice (Fig. 3 D and not depicted), suggesting an activated phenotype. To test whether LMP1/CD40-expressing

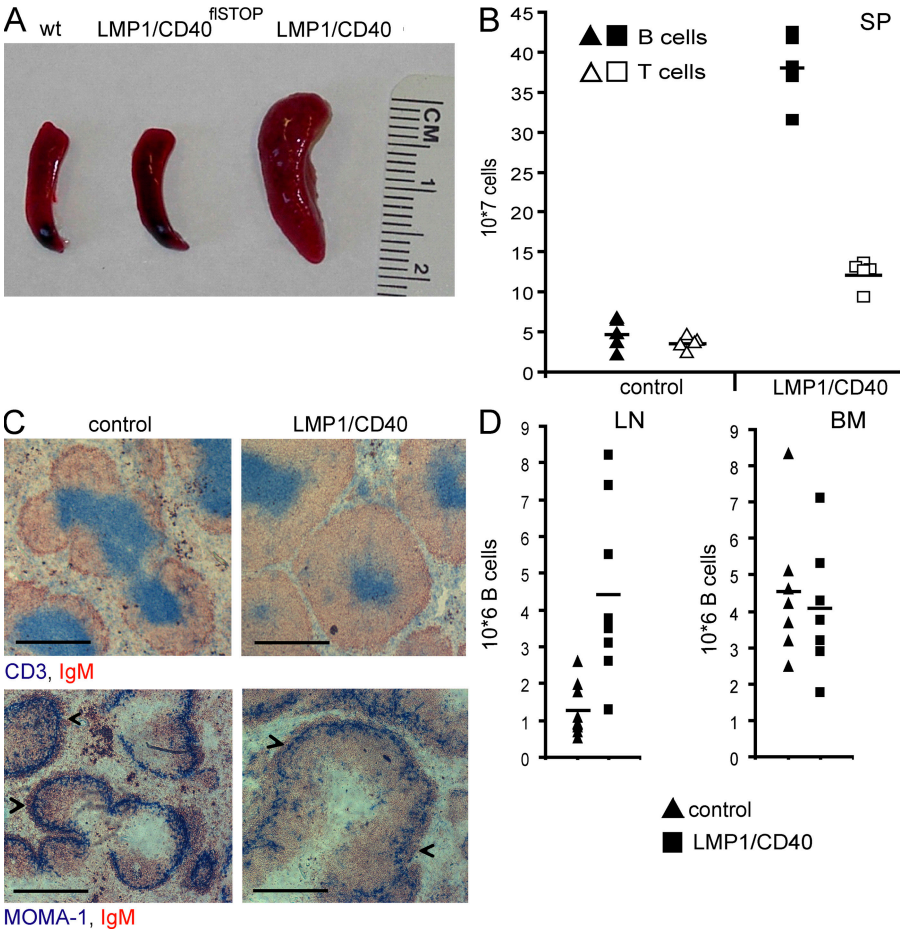

Figure 2. B cell–specific LMP1/CD40 expression results in an increase in B and T cell numbers in secondary lymphoid organs. (A) LMP1/CD40 mice showed a splenomegaly with a 3.5-fold increase of the splenic weight compared with control mice with B cells carrying the stop cassette (LMP1/CD40^{flSTOP}). Representative spleens from 8-wk-old LMP1/CD40 and control mice are shown. (B) Absolute numbers of B220$^+$ B cells and CD3$^+$ T cells in spleen (SP) of LMP1/CD40 and control mice. The horizontal bars mark the mean. (C) Spleen sections from LMP1/CD40 and control mice were stained for B cells (red, anti-IgM) and T cells (top; blue, anti-CD3), or for B cells (red, anti-IgM) and metallophilic macrophages (blue, anti-MOMA1), which are localized at the border between follicular (FO) and marginal zone (MZ) B cells (bottom). Arrowheads indicate marginal zone B cells. Bars, 400 µm. (D) Absolute numbers of B220$^+$ B cells in inguinal LN and BM of LMP1/CD40 and control mice. The horizontal bars mark the mean.

B cells could participate in TD immune responses, we immunized mice with the hapten (3-hydroxy 4-nitrophenylacetyl [NP]) conjugated to the carrier chicken gammaglobulin. In contrast to control mice, the fraction of GC B cells was drastically reduced in the spleens of LMP1/CD40 mice, and GC structures could not be detected by immunohistochemistry, suggesting that constitutive CD40 signaling impairs the recruitment and/or maintenance of B cells within GCs (Fig. S2, available at http://www.jem.org/cgi/content/full/jem.20080238/DC1).

As expected, T cells showed no deletion of the stop cassette, as analyzed by PCR (unpublished data), but were expanded and showed an activated phenotype in LMP1/CD40 mice. The ratio between CD4 and CD8 cells was comparable to the controls (unpublished data), but staining for CD44 and CD62L expression revealed a shift from naive toward activated and memory-type T cells among the CD4 and CD8 subsets (Fig. S3, available at http://www.jem.org/cgi/content/full/jem.20080238/DC1). These data indicate that both B and T cells were activated in LMP1/CD40 mice.

LMP1/CD40–expressing B cells proliferate spontaneously and have a prolonged survival in vitro

To determine the survival properties of LMP1/CD40-expressing and control B cells, we cultured such cells for 5 d in the presence or absence of α-CD40. The cells were stained daily with the vital dye TOPRO-3, and then subjected to flow cytometric analysis (Fig. 4 A). The percentage of living cells dropped dramatically in control culture in the absence of CD40 stimulation, whereas the same culture conditions only modestly affected the viability of LMP1/CD40-expressing cells. Furthermore, absolute numbers of living cells were determined for LMP1/CD40-expressing cells and controls over time (Fig. 4 B). An increase in the number of

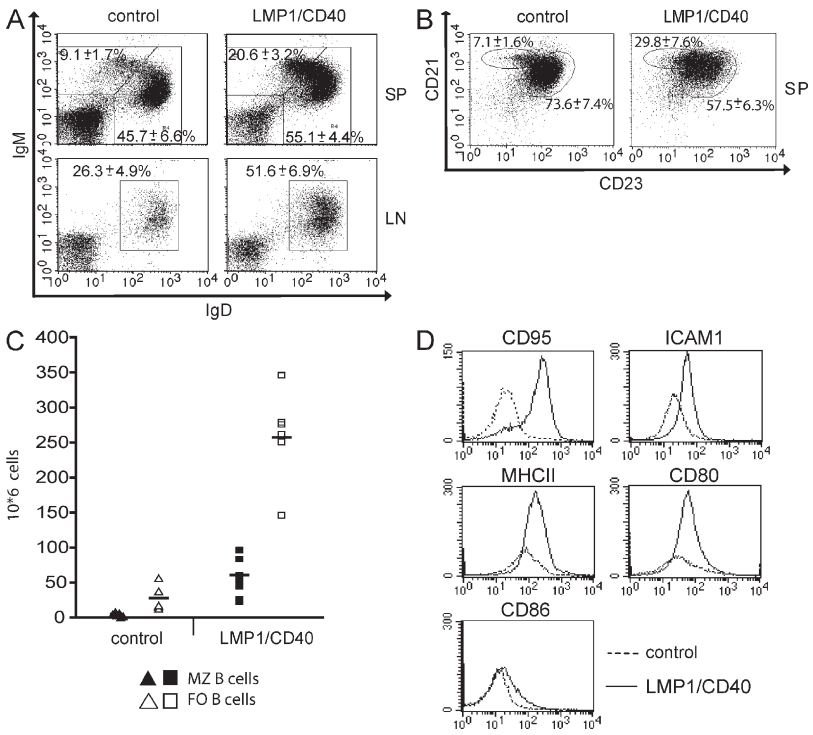

Figure 3. B cell–specific expression of LMP1/CD40 results in an increase and activation of B cells. (A) Lymphocytes of spleen (SP) and inguinal LNs were analyzed for the expression of IgM and IgD by flow cytometry. Numbers indicate the mean percentages and SD of gated populations. SP: follicular (FO) B cells (IgM^+IgD^+), marginal zone (MZ), and transitional B cells (IgM^+IgD^{low}); LN: IgM^+IgD^+. Values were calculated from seven independent experiments. (B) Flow cytometric analysis of follicular B cells (FO; $CD21^{int}CD23^+$) and marginal zone B cells (MZ; $CD21^{high}CD23^{low}$) in the spleen. Numbers indicate mean percentages and standard deviations of $B220^+$ B cells displaying a MZ B or FO B cell phenotype. Values were calculated from seven independent experiments. (C) Absolute numbers of FO and MZ B cells in the spleens of LMP1/CD40 and control mice. (D) Splenocytes were stained with antibodies specific for the indicated activation and adhesion markers. Histograms show surface expression of the indicated markers on gated $B220^+$ B cells from LMP1/CD40 (continuous line) and control (dotted line) mice. Lymphocytes isolated from LNs showed a similar extent of activation (not depicted).

LMP1/CD40-expressing cells was observed even without additional stimulation, indicating not only better survival but also spontaneous cell division. Additionally, B cells of LMP1/CD40 mice and controls were labeled with CFSE, cultured with or without α-CD40, IL-4, α-CD40 plus IL-4, or LPS, followed by flow cytometric analysis after 5 d (Fig. 4 C). Compared with control cells, a higher percentage of LMP1/CD40-expressing cells proliferated in the absence of exogenous stimuli or after stimulation with IL-4. Triggering of CD40 resulted in increased proliferation of control B cells, which could be further increased by the addition of IL-4, whereas proliferation of LMP1/CD40-expressing cells was not increased upon CD40 cross-linking. Proliferation upon LPS stimulation was comparable in both cell types.

B cell–specific expression of LMP1/CD40 activates the MAPKs Jnk and Erk and the noncanonical NF-κB pathway

Because it has been shown that cross-linking of the CD40 receptor induces activation of the MAPKs Erk, Jnk, and p38/MAPK (1, 6), the phosphorylation status of these proteins was tested by Western blot analysis. The phosphorylated forms of Jnk and Erk were increased by approximately four- to sixfold in unstimulated LMP1/CD40-expressing B cells compared with control cells. In contrast, no significant change in the level of phosphorylated p38/MAPK could be detected in untreated transgenic B cells (Fig. 5, A and B). Upon cross-linking of the endogenous CD40 receptor, the activation of the MAPKs was further increased in LMP1/CD40-positive cells, although to a lower extent compared with control cells (Fig. 5 B). To evaluate whether improved survival of LMP1/CD40-expressing B cells requires activation of the MAPK pathways, we cultured LMP1/CD40-expressing and control B cells in the presence of the Mek1/2 inhibitor U0126 and the Jnk inhibitor SP600125, preventing the phosphorylation of Erk and the kinase activity of Jnk, respectively (28, 29). The Mek1/2 inhibitor abrogated the improved survival of ex vivo–isolated LMP1/CD40-expressing B cells, whereas the Jnk inhibitor had a less dramatic effect (Fig. 5 C). These data suggest that the enhanced survival mediated by LMP1/CD40 is more dependent on Erk than Jnk activity.

Because CD40-induced B cell proliferation and survival critically depend on the activation of NF-κB (22), the canonical and noncanonical NF-κB signaling pathways were analyzed in LMP1/CD40-expressing B cells. In gel retardation assays, both unstimulated LMP1/CD40-expressing and control B cells exhibited similar amounts of p50/p65 complexes

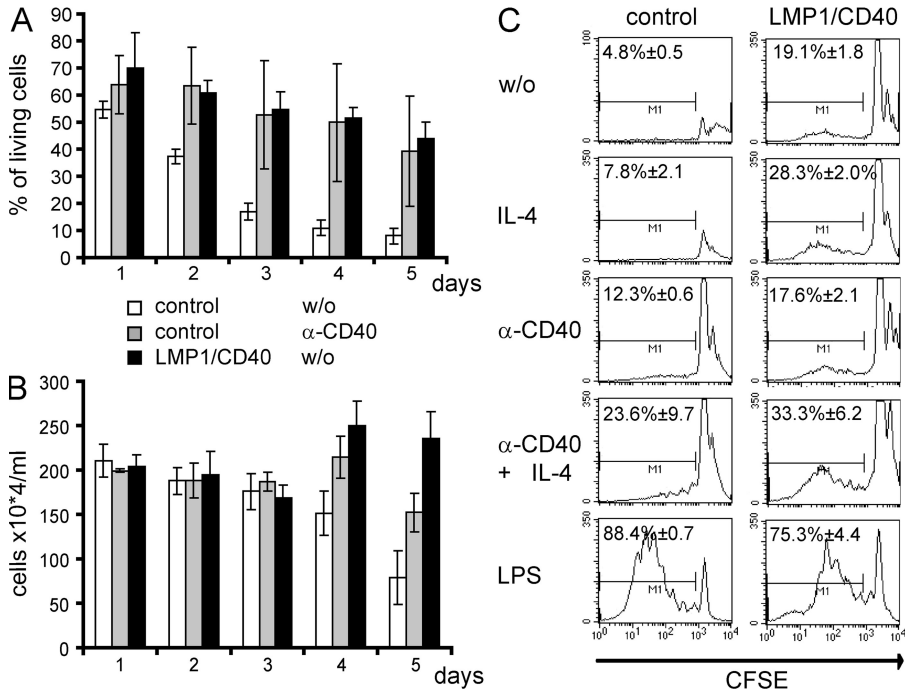

Figure 4. LMP1/CD40 expression triggers survival and spontaneous proliferation of primary B cells in vitro. Splenic B cells of LMP1/CD40 and control mice were enriched by depletion of CD43+ cells. Cells were cultured for up to 5 d with anti-CD40 antibody (α-CD40) or without stimulation (w/o). (A) Percentages of living cells (Topro negative) were determined daily by flow cytometry. The bars show mean percentages of living cells of three independent experiments. Error bars show the SD. (B) Numbers of viable cells were determined daily by trypan blue staining and cell counting. The bars show mean cell counts of three independent experiments. Error bars show the SD. (C) Splenic B cells of LMP1/CD40 and control mice were labeled with CFSE and cultured with α-CD40, IL-4, α-CD40 plus IL-4, LPS, or without stimulation (w/o). After 5 d of culture, the proliferation rate of B220+ B cells was determined by flow cytometric analysis of the CFSE staining. Percentages of divided cells ± the SD of three individual experiments are indicated.

(Fig. 6 A and Fig. S4 A, available at http://www.jem.org/cgi/content/full/jem.20080238/DC1). Stimulation of the endogenous CD40 receptor resulted in a robust induction of DNA-binding p50/p65 complexes in control cells. This extent of induction could be seen in neither unstimulated nor in α-CD40–stimulated LMP1/CD40-expressing B cells (Fig. 6 A and Fig. S4 A). These data indicate that the canonical NF-κB signaling pathway is not constitutively activated in LMP1/CD40-expressing cells. The data were confirmed by Western blot analysis showing that IκB-α levels were comparable in control and LMP1/CD40-expressing B cells, and that IκB-α was not constitutively phosphorylated in unstimulated LMP1/CD40 B cells. As shown in Fig. 6 B, IκB-α was even less phosphorylated in unstimulated LMP1/CD40-expressing cells than in control B cells. Inhibition of de novo IκB-α synthesis by addition of cycloheximide excluded the possibility that pIκB-α cannot be detected in the Western blots because of an increased high turnover rate of IκB in unstimulated LMP1/CD40-expressing B cells (Fig. S4 B). Upon CD40 stimulation, degradation of IκB-α in B cells expressing LMP1/CD40 was delayed in comparison to control cells, indicating that in mutant cells the canonical NF-κB signaling pathway can be activated, but to a lower extent than in control cells (Fig. S4 B). In contrast to control cells, we could detect a RelB-containing complex in LMP/CD40-positive B cells in gel retardation assays (Fig. 6 A). Furthermore, in Western blots, increased p52 protein levels could be detected in mutant B cells compared with control B cells, whereas p100 levels were comparable (Fig. 6 B), thus indicating constitutive activation of the noncanonical NF-κB signaling pathway.

To corroborate these findings, we analyzed the protein levels of NF-κB components in the cytoplasm and nucleus. In accordance with the previous results, the levels of RelB and p52 were elevated, whereas p65 and c-Rel levels were similar in nuclear fractions of LMP1/CD40 and control cells (Fig. 6 C). However, c-Rel levels were significantly decreased in the cytoplasm of LMP1/CD40-expressing B cells. Additionally, a significant increase in p50 levels was found in nuclear extracts of LMP1/CD40-expressing cells, which is most likely caused by the increased p105 levels found in the cytoplasm. The increased p50 level might lead to the formation of p50/p50 homodimers, lacking a transactivation domain. It has been shown that, in tumor cells, p50/p50 homodimers interact with Bcl3, resulting in transcriptional activation of NF-κB target genes. This is mostly correlated with elevated Bcl3 levels. However, in LMP1/CD40-expressing cells we could detect neither increased levels of p50/p50 homodimer formation in gel retardation assays (Fig. S4 A) nor elevated Bcl3 levels in the nuclear fraction (Fig. 6 C), suggesting that most p50 is bound to RelB and thereby contributes to the

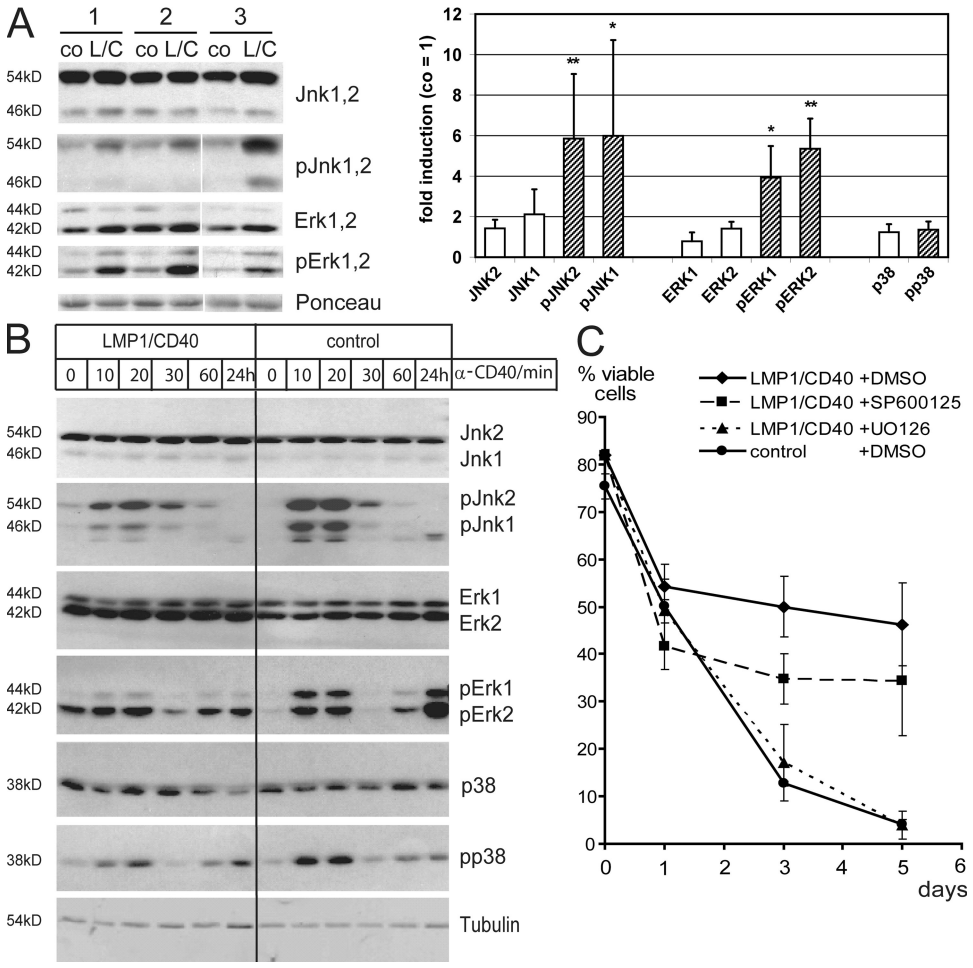

Figure 5. LMP1/CD40 expression induces activity of the Jnk- and Erk-signaling pathways. (A) Whole-cell extracts of splenic B cells of LMP1/CD40 (L/C) and control (co) mice from three independent preparations (1–3) were loaded on one gel and analyzed for Jnk (Jnk2, 54 kD; Jnk1, 46 kD), Erk (Erk1. 44kD; Erk2, 42 kD), p38/MAPK (38 kD) and the corresponding phosphorylated forms with specific antibodies. Equal protein loading was controlled by Ponceau S staining. The graph shows the mean values of the fold induction of the signals from the unphosphorylated and phosphorylated forms of Jnk, Erk, and p38/MAPK compared with the signals in control cells. Mean values and SDs were calculated from at least five independent experiments. SDs are shown by error bars. *, $P < 0.05$; **, $P < 0.001$, calculated by the two-tailed Student's *t* test. (B) After CD40 triggering, LMP1/CD40-expressing cells are damped in activation compared with control cells. Splenic B cells of LMP1/CD40 and control mice were stimulated with α-CD40 antibody for the indicated time points, and Western blots were performed as described in A. Equal protein loading was controlled by tubulin staining. One representative experiment out of three is shown. (C) The improved survival of LMP1/CD40-expressing B cells is dependent on continuous Erk phosphorylation. Splenic B cells of LMP1/CD40 and control mice (CD19-Cre) were cultured for up to 5 d with the Mek1/2 inhibitor U0126 (dotted line) and the Jnk-inhibitor SP600125 (dashed line; triangle and square, respectively). As control, B cells from LMP1/CD40 and control mice were cultured in the presence of DMSO (continuous lines, rectangle, and circle, respectively). Percentages of living cells (Topro negative) were determined by flow cytometry at day 1, 3, and 5. The bars show mean percentages of living cells of three independent experiments. Error bars show the SD.

activity of the noncanonical NF-κB signaling pathway. Collectively, these results indicate that constitutive activation of CD40 favors the activation of the noncanonical NF-κB signaling pathway.

LMP1/CD40 mice develop B cell lymphomas

Because LMP1/CD40-expressing B cells exhibited spontaneous proliferation and enhanced survival in vitro, which might ultimately lead to the development of malignancies, we monitored the mice for the occurrence of B cell lymphomas by regularly palpating the abdomen. A high percentage of LMP1/CD40-expressing mice older than 12 mo showed obvious signs of disease. Those mice were further analyzed and showed an extreme splenomegaly with a 20–40-fold increase in weight, significantly enlarged inguinal LNs, hepatomegaly, and nodular infiltrates in the kidney, lung, and liver (Fig. S5, available at http://www.jem.org/cgi/content/full/jem.20080238/DC1).

To confirm lymphoma development in these mice, splenic cells were analyzed for mono- or oligoclonality by Southern blot analysis using a probe spanning the J_H3-4 region of the mouse IgH locus. In contrast to the controls, all spleen cell

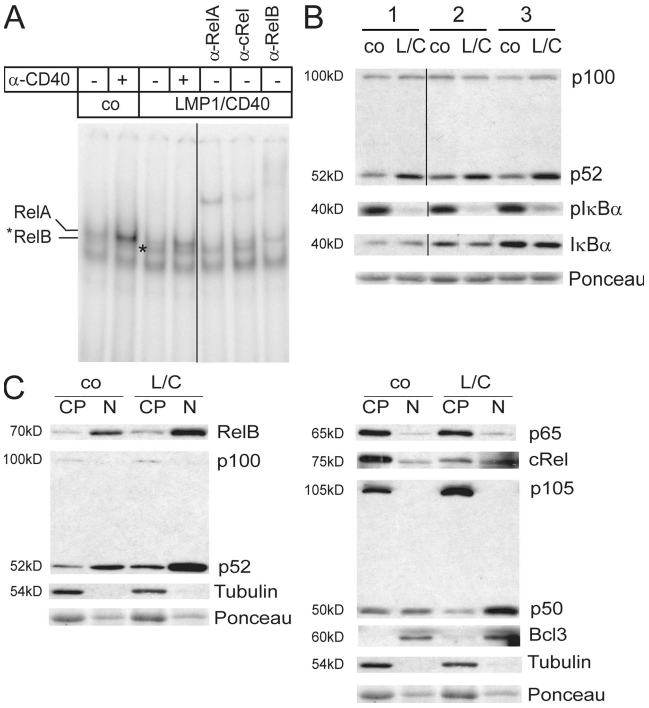

Figure 6. LMP1/CD40 expression induces activity of the noncanonical NF-κB pathway. (A) Splenic B cells of LMP1/CD40 and control (co) mice were cultured with (+) or without (−) α-CD40 for 1 h. Nuclear extracts were incubated with radioactively labeled DNA oligonucleotides containing a NF-κB binding site and separated by gel electrophoresis. For supershift experiments, the indicated antibodies were added to the extracts. (B) Whole-cell extracts of splenic B cells of LMP1/CD40 and control (CD19-Cre) mice from three independent preparations (1–3) were loaded on one gel and analyzed by immunoblot. The expression levels of p100 and p52 as well as of IκBα and pIκBα are shown. Equal protein loading was verified by Ponceau S staining. (C) Cytoplasmic (CP) and nuclear (N) levels of NF-κB components of splenic B cells from LMP1/CD40 and control (CD19-Cre) mice were analyzed by immunoblot. Purity of cytoplasmic and nuclear extracts was verified by α-tubulin and α-Bcl3 staining, respectively. Equal protein loading was controlled by Ponceau S staining. The experiment was performed three times.

samples of diseased LMP1/CD40 mice showed beside the germline IgH band one or more distinct additional bands, indicating a mono- or oligoclonal outgrowth of B cells (Fig. 7 A). This was further confirmed by the sequence analysis of the CDR3 region (Fig. S6, available at http://www.jem.org/cgi/content/full/jem.20080238/DC1). Whereas several rearrangements could be amplified in wild-type cells, only one or two rearrangements were amplified from the tumor samples. None of the lymphomas carried IgH somatic mutations. The tumors were further characterized by immunohistopathology and FACS analysis. Hematoxylin and eosin (HE) staining of spleen sections showed a nodular infiltrate characterized by the presence of small and large lymphoid cells that could not be seen in the controls (Fig. 7 B). Nine tumors were further analyzed by immunohistochemical stainings. Staining for B220 and CD3 surface markers demonstrated that in seven cases, the expanded population was

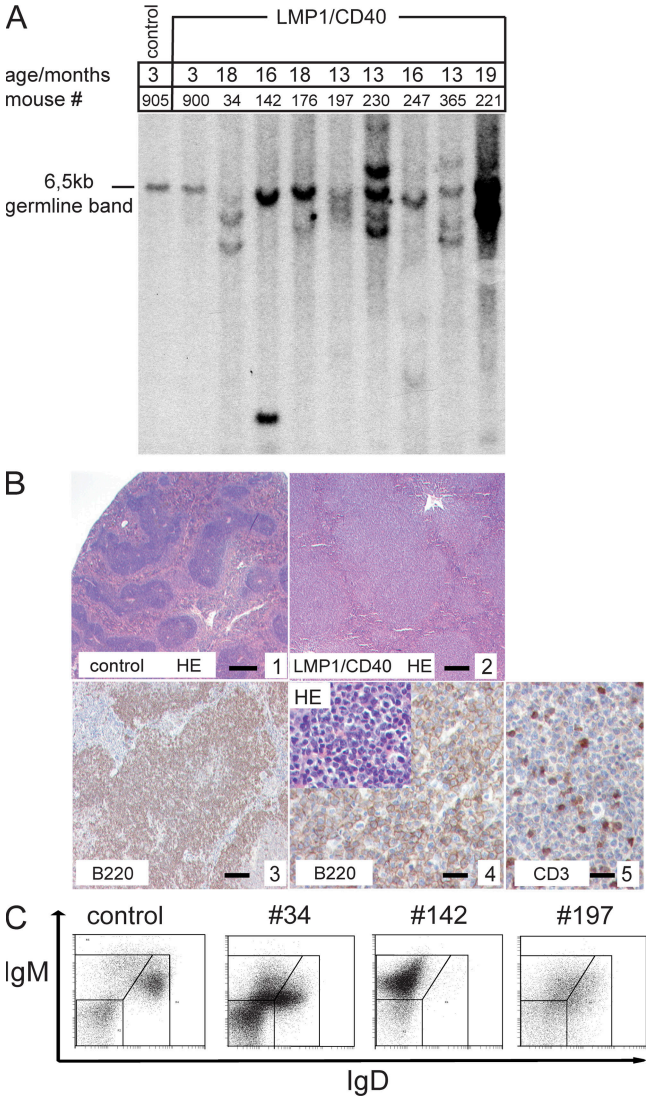

Figure 7. LMP1/CD40 mice develop mono- and oligoclonal lymphomas. (A) Southern blot analysis to examine IgH gene configuration with an IgH-specific probe. Genomic DNA was prepared and digested with EcoRI from splenic cells of LMP1/CD40 mice that developed neoplasias (34, 142, 176, 197, 230, 247, 365, and 221), one young LMP1/CD40 mouse (900; 3 mo of age), as well as a control mouse (905). The sequence analysis of the amplified IgH genes is shown in Fig. S6. (B) Representative histological analyses of diseased LMP1/CD40 mice and age matched control mice. (1) HE-stained normal spleen. (2) HE-stained spleen representative for diseased LMP1/CD40 mice, showing prominent nodular tumor infiltrates. (3) Lymphoma infiltrate within the spleen of a representative diseased LMP1/CD40 mouse. B cells were visualized by immunohistochemistry using an antibody specific for B220. (4) Higher magnification of section described in 3. (5) Dispersed reactive T cells within the lymphoma infiltrate were detected by an anti-CD3–specific antibody. A representative highly magnified section is shown. Bars: (1 and 2) 400 µm; (3) 100 µm; (4, 5, and inset) 25 µm. (C) Flow cytometric analysis of splenic cells for the expression of IgM and IgD. The gates were set according to the age-matched controls. For the diseased LMP1/CD40 mice, a shift toward one or two main populations could be observed, as shown for three representative samples. Fig. S6 is available at http://www.jem.org/cgi/content/full/jem.20080238/DC1.

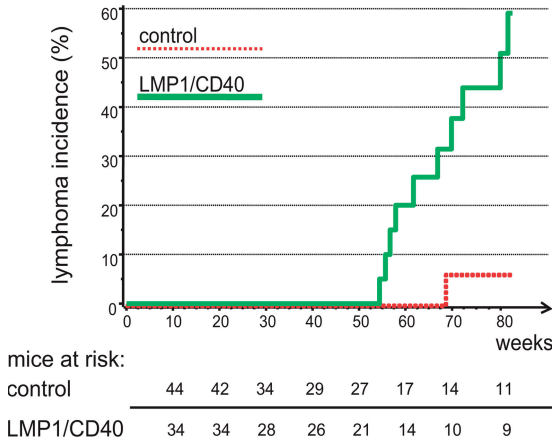

Figure 8. LMP1/CD40 mice develop lymphomas with a high incidence. Kaplan-Meier curve for lymphoma incidence in LMP1/CD40 and control mice. Lymphomas were scored by histopathology and by investigating mono-/oligoclonality, using Southern blot analysis and/ or PCR amplification of the immunoglobulin genes, followed by sequence analysis. Reduction of the control group between 50 and 80 wk is caused by the analysis of these mice. At each time point, a diseased LMP1/CD40 mouse was analyzed, an age-matched control mouse was included. Dropouts that were caused by nonlymphoma-derived death were equal in both groups. In the age between 12 and 19 mo, 11/19 LMP1/CD40-mice and 1/14 control mice developed tumors, respectively.

composed of $B220^+CD3^-$ B cells (Fig. 7 B). In two $B220^-$ cases, B cell derivation of the expanded cell population could be confirmed by staining for the B cell markers Pax5/BSAP and CD79a (unpublished data). Within the expanded B cell population, small $CD3^+$ T lymphocytes could be detected (Fig. 7 B).

Further analysis of the B cell populations in spleen, LN, peritoneal cavity, and BM by FACS analysis revealed an aberrant B cell population in most cases, which was either IgM^+IgD^- or $IgM^{low}IgD^+$, and a strong reduction of the normal IgM^+IgD^{high} population (Fig. 7 C). In one case, we observed a selective outgrowth of $CD4^+$ T cells. The B cell lymphomas were heterogenous in the expression of CD95, but all showed a strong down-regulation of CD21 and CD23 (Fig. S7 A, available at http://www.jem.org/cgi/content/full/jem.20080238/DC1). None of the tumor cells tested showed a significant up-regulation of LMP1/CD40 expression compared with premalignant cells (Fig. S7 B).

To determine the activity of NF-κB and MAPK in tumor cells, we performed Western blot analysis. We could detect elevated p52 levels in three out of seven tumor samples tested. (Fig. S8, A and B, available at http://www.jem.org/cgi/content/full/jem.20080238/DC1). In three out of seven tumor samples, pIκB-α levels were increased compared with premalignant LMP1/CD40-expressing cells. Approximately 25% (2/7) and 90% (6/7) of tumor samples displayed constitutive Jnk and Erk phosphorylation, respectively. These data indicate that distinct signaling pathways are activated in the various tumor samples, suggesting that different secondary events drive B cell transformation (Fig. S8, A and B).

Scoring lymphoma development by immunohistopathological and molecular analyses revealed that approximately 60% (11/19) of LMP1/CD40 mice between the age of 12 and 19 mo developed lymphomas, whereas the frequency of lymphoma development in the control population was <10% (1/14; Fig. 8). These data show that deregulated CD40 expression in B cells leads to a high incidence of lymphoma development in mice.

DISCUSSION

Deregulated CD40 signaling has been described in several human malignancies (18). Yet, the question of whether aberrant CD40 signaling is sufficient to promote tumorigenesis remains unresolved. To investigate biological and pathological roles of constitutive CD40 signaling in B cells, we used the transmembrane domain of LMP1 as a surrogate to induce ligand-independent aggregation of the CD40 intracellular signaling domain. We show that constitutive CD40 signaling in B cells leads to a significant increase in peripheral mature B cells and, ultimately, to the development of mature B cell lymphomas.

Previous in vitro experiments have shown that the LMP1/CD40 fusion protein acts similar to LMP1 in terms of self-aggregation and is able to mimic ligand-triggered CD40 signaling with respect to the activation of NF-κB and stress-activated protein kinases (23, 24). In this study, we show that B cell–specific LMP1/CD40 expression in transgenic mice can replace CD40–CD40L interaction to promote immunoglobulin class switching, thus indicating that LMP1/CD40 indeed acts as a constitutively active CD40 receptor. B cell–specific expression of LMP1/CD40 in mice caused splenomegaly with an accumulation of both follicular and marginal zone B cells. The expansion of transgenic B cells may depend on their prolonged survival and/or increased proliferation as demonstrated by our ex vivo studies and in vivo BrdU incorporation assays (Fig. 6 and unpublished data). Despite their activated status, transgenic B cells were strongly impaired in GC formation. This is in accordance with a previous study showing that LMP1/CD40 is able to down-regulate *bcl6*, which is a key regulator of the GC reaction (30). We observed not only an accumulation of B cells but also of activated $CD4^+$ and $CD8^+$ T cells in young LMP1/CD40 mice. It is unlikely that this T cell expansion is caused by a leakiness of Cre recombinase expression because the same T cell expansion was observed in crossings with two independent B cell–specific Cre lines (CD19-Cre and CD21-Cre). Additionally, deletion of the stop cassette in T cells of LMP1/CD40 mice could not be detected by PCR (unpublished data). Therefore, the observed T cell expansion might instead be caused by an antigen-independent bystander effect induced by LMP1/CD40-expressing B cells. It has been shown that production of cytokines, as well as cell surface molecules, expressed on antigen-presenting cells during an immune response can activate T cells nonspecifically (31, 32), and that CD40-activated antigen-presenting cells promote the expansion of memory T cells (33, 34), suggesting that LMP1/CD40-expressing

B cells may be able to generate an activating environment for T cells.

Deregulated CD40 signaling induced the development of lymphomas in >60% of mice older than 1 yr. Consistent with the B cell–specific expression of LMP1/CD40 and the effects of constitutive CD40 signaling on B cell survival and proliferation, most of these tumors were of clonal B cell origin. Only 1 out of 11 lymphomas was T cell derived. In all other tumors, the expanded population carried clonal IgH rearrangements and expressed B cell markers. The nodular growth pattern of the lymphomas was reminiscent of follicular lymphomas (35). However, in contrast to follicular lymphomas, the variable regions of the immunoglobulin genes cloned from LMP1/CD40-expressing B lymphoma cells were unmutated, indicating a pre-GC origin. The late onset of tumor development, the heterogeneity in surface marker expression, and the activity of distinct signaling pathways suggest that multiple independent secondary oncogenic hits cooperate with CD40 activation to promote lymphomagenesis.

A role for CD40 signaling in the pathogenesis of human B cell lymphomas and carcinomas has previously been suggested. We provide strong evidence that constitutive CD40 signaling exerts transforming activity in vivo. The oncogenic property of constitutive CD40 signaling appears in contrast with the previously reported therapeutic effects of CD40 triggering in hematopoietic malignancies (18, 36). Indeed, triggering the CD40 receptor can promote growth arrest and cell death of malignant CD40-expressing cells and can induce an autologous antitumor T cell response by up-regulating the costimulatory molecules B7.1 and B7.2 (37). Our data suggest that this therapeutic approach might not be risk free. The level and duration of the CD40 signal may critically influence the balance between the apparently contrasting biological effects triggered by CD40 signaling. Indeed, low-level constitutive engagement of CD40 was shown to induce proliferation of lymphoma cells, whereas treatment of malignant cells with high doses of agonistic anti-CD40 antibodies or CD40L resulted in cell cycle arrest and apoptosis (20).

Our gel retardation and nuclear fractionation experiments revealed that, compared to control B cells, RelB-containing complexes are increased in the nuclei of LMP1/CD40-expressing B cells, indicating constitutive activation of the noncanonical NF-κB pathway. We suggest that in LMP1/CD40-expressing B cells, RelB dimerizes with either p50 or p52, which were both found to be increased in the nuclear fraction. This is in accordance with previous reports showing that the noncanonical NF-κB pathway based on p100 processing leads to the nuclear translocation of not only RelB/p52 but also of RelB/p50 dimers (17, 38). In contrast to the noncanonical pathway, the canonical NF-κB pathway was not found to be activated in LMP1/CD40-expressing B cells, as indicated by similar p65 and c-Rel levels in the nuclear fractions of unstimulated LMP1/CD40-expressing B cells and control B cells. The reduced basal phosphorylation of IκB-α in LMP1/CD40-expressing B cells compared with control B cells suggests that the canonical NF-κB pathway is even less active in the mutant cells than in unstimulated control B cells. Additionally, in comparison to control B cells, p105 levels were increased, whereas c-Rel levels were decreased, in the cytoplasm of LMP1/CD40-expressing B cells. Whether this alteration is caused by the constitutive activation of CD40 or a direct consequence of the constitutively activated noncanonical NF-κB pathway remains to be determined. The question arises why LMP1/CD40 expression in B cells leads selectively to the activation of the noncanonical NF-κB pathway. In wild-type B cells, CD40 ligation results in a fast and robust activation of the canonical NF-κB activity, which is rapidly counteracted by multiple negative-feedback mechanisms, whereas the noncanonical NF-κB pathway responds more slowly and appears to lack strong negative-feedback mechanisms (39). This might explain the preferential chronic activation of the noncanonical NF-κB pathway in LMP1/CD40-expressing B cells. Recently, two studies have provided compelling evidence that the noncanonical NF-κB pathway plays a critical role in multiple myeloma (MM) pathogenesis (40, 41). Thus, 20% of patients with MM were found to carry mutations in essential NF-κB components, leading mainly to the activation of the noncanonical NF-κB pathway (41). Of note, in some cases of MM, a strong up-regulation of CD40 was observed. As shown for CD30 (42), CD40 overexpression might lead to self-aggregation of CD40, resulting in ligand-independent constitutive CD40 signaling, and thus creating a primary oncogenic event similar to that seen in our experimental system.

In addition to the noncanonical NF-κB pathway, the MAPKs Erk and Jnk were constitutively phosphorylated in unstimulated LMP1/CD40-expressing B cells. The importance of Erk phosphorylation for the improved survival of ex vivo–isolated LMP1/CD40-expressing B cells was supported by the fact that the survival advantage by LMP1/CD40 expression was abrogated in the presence of the Mek1/2 inhibitor UO126. The Ras–Raf–Mek–Erk pathway has been implicated in malignant transformation of various cell types and has been associated with proliferation and survival of hematopoietic cells (43). A basal constitutive activity of Erk, which has been attributed to CD40, CD30, and RANK signaling, has also been described in the Hodgkin-Reed Sternberg tumor cells of Hodgkin disease (44). Treatment of Hodgkin disease cell lines with the MEK inhibitor UO126 resulted in the inhibition of proliferation, underlining the importance of constitutive Erk phosphorylation for the proliferation of Hodgkin lymphoma cell lines. Unlike premalignant LMP1/CD40 B cells, constitutive Erk phosphorylation was not consistently detected in all independent primary tumors derived from LMP1/CD40-expressing B cells. This result suggests the existence of distinct oncogenic partners involved in CD40-driven lymphomagenesis, some of which may bypass the need for Erk activation.

Our results provide direct evidence that constitutive CD40 signaling leads to the selective activation of the noncanonical NF-κB pathway and the MAPKs Jnk and Erk. The concerted action of these signaling pathways ultimately leads

to B cell lymphomagenesis. The mouse model described in this paper provides a tool to dissect the contribution of these signaling pathways to lymphomagenesis in vivo.

MATERIALS AND METHODS

Generation of the transgenic mouse line LMP1/CD40. The *LMP1/CD40* chimeric gene was isolated from the plasmid p1778.16 encoding aa 1–190 from LMP1 fused to aa 223–280 of human CD40 (23). The adenine at position 243 bp after the ATG of the LMP1 gene was replaced by a cytosine, introducing a silent mutation, to destroy a potential splice acceptor side. To insert the *LMP1/CD40* fusion gene into the *rosa26*-locus, the vector pRosa26-1 was used (45). Before introducing *LMP1/CD40*, pRosa26-1 was modified by introducing a loxP-flanked region, consisting of a stop cassette containing a transcription and translation termination site (46), the gene encoding the red fluorescent protein (not expressed in this context), and a neomycin-resistance gene flanked by frt sites. The *LMP1/CD40* fusion gene was cloned downstream of the stop cassette. The final targeting vector was electroporated into BALB/c-derived ES cells. The targeted ES cells were screened for homologous recombination by Southern blot analysis. The DNA was digested with EcoRI and hybridized with a specific *rosa26* probe (45). Recombinant ES cells were injected into C57BL/6 blastocysts, which were then transferred into foster mothers to obtain chimeric mice.

Mice. Mice carrying the *LMP1/CD40^{flSTOP}* allele were crossed either to the CD19-Cre or the CD21-Cre mouse strain (on a C57BL/6 background) to generate mice expressing the transgene in early B cell stages in the BM ([LMP1/CD40^{flSTOP};CD19-Cre] F1) or in mature B cells ([LMP1/CD40^{flSTOP};CD21-Cre] F1), respectively. Offspring were routinely screened by PCR using primer specific for *LMP1/CD40* (5′LMP1, 5′-AGGAGCCCTCCTTGTCCTCTA-3′; 3′CD40, 5′-CTGAGATGCGACTCTCTTTGCCAT-3′) and *CD19-Cre* or *CD21-Cre* (26, 27).

Only mice of the F1 generation were used in this study and analyzed at 8–16 wk of age unless stated otherwise. As controls, LMP1/CD40^{flSTOP} and CD19-Cre– or CD21-Cre–expressing mice were used. All mice were bred and maintained in specific pathogen-free conditions, and the experiments were performed in compliance with the German animal welfare law and have been approved by the institutional committee on animal experimentation and the government of Upper Bavaria.

Western blot. 3×10^6 cells were lysed in Laemmli buffer or NP40 lysis buffer, and lysates were separated on a SDS-PAGE gel and transferred to a nitrocellulose or PVDF membrane. LMP1/CD40 protein was detected by the anti–human CD40 antibody (sc975), which was like anti–IκB-α (sc-371), purchased from Santa Cruz Biotechnology, Inc. MAPKs and their phosphorylated forms were detected by anti-p38/MAPK, anti–phospho-p38/MAPK (pT180/pY182), anti-Erk (p44/42), anti–phospho-Erk (pT202/pY204), anti-Jnk (56G8), and anti–phospho-Jnk (pT183/pY185), all purchased from Cell Signaling Technology. The phosphorylated form of IκB-α was detected by anti–phospho-IκB-α (Cell Signaling Technology). Signals were visualized with ECL Western Blotting Detection Reagents (GE Healthcare). The amount of loaded protein was standardized against tubulin using an anti-tubulin antibody (Dianova). After scanning of the films with an Expression 1680Pro scanner (Epson), quantification of bands was performed with the TINA software package (Raytest). Protein expression values of control mice were set to 1 to achieve comparability between different Western blots. P values were determined by applying the two-tailed Student's *t* test.

In vitro cultures. Splenic cells were cultured for up to 5 d in 96-well plates (5×10^5 cells/well). Stimuli included lipopolysaccharide (20 μg/ml; *Escherichia coli* 055:B5; Sigma-Aldrich), IL-4 (10 ng/ml; mouse recombinant; Sigma-Aldrich), and anti-CD40 antibody (10 μg/ml; BD Biosciences; 3/23). Cells were stained and analyzed with a FACSCalibur or counted using trypan blue to exclude dead cells. For proliferation assays, splenic cells (5×10^6 cells/ml) were labeled by incubation in serum-free RPMI media containing CFSE (final concentration 5 μM; Invitrogen) for 10 min at 37°C. CFSE-labeled cells were cultured for up to 5 d in 96-well plates (5×10^5/well) in B cell medium and analyzed by flow cytometry. For treatment with small chemical inhibitors, B cells were cultured with 2.5 μM SP600125 (Ag Scientific), 10 μM UO126 (Cell Signaling Technology), or DMSO (Calbiochem) in B cell medium for up to 5 d.

For Western blots and gel retardation assays, B cells were purified from spleen, using magnetic beads against CD43 (MACS; Miltenyi Biotec), and stimulated from 5 min for up to 24 h with agonistic anti-CD40 antibodies (10 μg/ml; J Bioscience [HM40-3]). For IκB-α degradation assays, B cells were treated with 10 μM cycloheximide (Sigma-Aldrich) 30 min before stimulation.

Tumor cells. Primary tumor cells were frozen in RPMI, 10% DMSO, and 20% FCS. Because all tumor cells are CD43$^+$, we were not able to purify them with magnetic beads as we did for premalignant cells. Therefore, after thawing, cells were cultured for 2 d to obtain a purer tumor cell population before Western blots extracts were prepared.

Flow cytometry. Single-cell suspensions prepared from various lymphoid organs were surface stained with combinations of FITC, PE, Cy-Chrome (Cyc), APC, and Cy5.5-conjugated monoclonal antibodies. Antibodies to B220, CD4, CD5, CD8, CD21, CD23, CD43, CD44, CD80, CD95, IgD, IgG1, and IgM were purchased from BD Biosciences and the antibody to CD62L was purchased from Immunotech. Additional monoclonal antibodies to CD54 and CD86 were provided by J. Mysliwietz (Helmholtz Center, Munich, Germany). Peanut agglutinin–FITC was purchased from Vector Laboratories. All analyses were made with a FACSCalibur (BD Biosciences) and results were analyzed using CellQuest software. Data were analyzed from 3×10^4 viable lymphocyte-gated cells as determined by forward and side scatter and propidium iodide or Topro-3 (Invitrogen) staining.

Immunohistochemistry. Spleens were embedded in OCT Tissue-Tek (Sakura), frozen on dry ice, and cut into 8-μm-thick sections. The sections were thawed, air dried, fixed in acetone, and incubated for 30 min at 22°C in a humidified chamber with anti-biotin, anti-avidin solution (Avidin/Biotin blocking kit; Vector Laboratories).

Sections were stained using peroxidase-conjugated anti–mouse IgM (Sigma-Aldrich), rat anti–mouse CD3 (provided by E. Kremmer, Helmholtz Center, Munich, Germany), and rat anti–mouse MOMA-1 (T-2011; BMA) antibodies. Biotin-conjugated mouse anti–rat IgG1 (Jackson ImmunoResearch Laboratories) was used to detect MOMA-1 or CD3 antibodies, and streptavidin coupled to alkaline phosphatase (Sigma-Aldrich) to detect the biotin-conjugated mouse anti–rat IgG1 antibody. Streptavidin-coupled antibodies were detected by the reaction with an alkaline phosphate substrate kit (Vector Laboratories), and peroxidase-coupled antibodies were detected by the reaction with 3-amino-9-ethylcarbazole (peroxidase substrate kit; Vector Laboratories). All incubation steps were performed at 22°C in humidified chamber, followed by three washing steps with PBS. Slides were analyzed with a microscope (Carl Zeiss, Inc.); pictures were obtained with a digital camera (RS Photometrics) and processed with Openlab (Improvision) and Photoshop (Adobe) software. Immunohistochemical staining of paraffin sections was performed on an automated immunostainer (Ventana Medical Systems) according to the manufacturer's protocols. Antigen retrieval was performed with a microwave pressure cooker in 0.01 M citrate buffer (pH 6.0). Incubation with the primary antibodies was performed overnight at room temperature. The rest of the procedure was completed on the Ventana immunostainer. The antibodies used included B220 (BD Biosciences), CD3 (Dako), Pax5 (BD Biosciences), and CD79a (clone HM57; Dako). Positive controls for all the antibodies investigated were used to confirm the adequacy of the staining.

Electrophoretic mobility shift assay. Nuclear protein extracts were prepared from stimulated and unstimulated cells, as previously described (47). The electrophoretic mobility shift assay was performed with a NF-κB–specific

double-stranded DNA probe, as previously described (48). For supershifts, 2 μg of specific antibodies against p50 (sc114), p65 (c20), c-Rel (sc70) p52 (sc298), and RelB (sc226) from Santa Cruz Biotechnology, Inc. were added to the binding reaction.

B cell fractionation. 2×10^7 B cells were incubated in 200 μl buffer A (10 mM Hepes, pH 7.9, 10 mM KCl, 0.1 mM EDTA, 0.1 mM EGTA, 1 mM DTT, and 1x complete protease inhibitors [Roche]) for 15 min on ice. After addition of 12.5 μl 10% NP-40 and shaking for 5 min at 4°C, nuclei were spun down at 15,000 rpm for 15 min, and the supernatant (cytoplasmic fraction) was saved. Nuclei were washed once with buffer A before lysis in buffer C (20 mM Hepes, pH 7.9, 0.4 M NaCl, 1 mM EDTA, 1 mM EGTA, 1 mM DTT, and 1x complete protease inhibitors). After shaking at 4°C for 30 min and centrifugation at 15,000 rpm for 15 min, the supernatant (nuclear fraction) was saved.

Analysis of lymphomas. Animals were kept under observation and palpated regularly to detect lymphoma development. Animals that were obviously sick were killed and analyzed. All animals were killed and analyzed at the age of 19 mo at the latest. Lymphomas were scored by histopathology and by investigating mono-/oligoclonality, using Southern blot analysis and/or PCR amplification of the immunoglobulin genes, followed by sequence analysis. Lymphoma incidences were estimated using the Kaplan-Meier method. Killed control mice or mice that died from causes unrelated to tumor development were defined as early dropouts. Statistical analysis was performed using the Statistical Analysis Software (SAS) version 6.12.

Analysis of IgH gene rearrangements. Genomic DNA was isolated from splenic cells, and Southern blot analysis with EcoRI-digested DNA was performed. To detect the IgH region, a radioactive-labeled J_H Probe was used representing the HindIII- and EcoRI-flanked 1.6-kb fragment spanning the J_H3-4 region of the mouse IgH locus.

Online supplemental material. Fig. S1 shows that LMP1/CD40 induces CSR to IgG1 in combination with IL-4. Fig. S2 shows that LMP1/CD40 impairs GC responses. Fig. S3 shows T cell activation by B cell–specific LMP1/CD40 expression. Fig. S4 shows preferential activation of the noncanonical NF-κB pathway by LMP1/CD40. Fig. S5 shows sequence analysis of the IgH CDR3 region. Fig. S6 shows tumors in LMP1/CD40 mice. Fig. S7 shows surface marker expression in LMP1/CD40 positive tumors. Fig. S8 shows signaling pathways in LMP1/CD40$^+$ tumors. The online version of this article is available at http://www.jem.org/cgi/content/full/jem.20080238/DC1.

We thank G.W. Bornkamm, N. Uyttersprot, and B. Jungnickel for critically reading the manuscript; D. Hölzel and M. Hölzel for help with the statistical analysis; W. Hammerschmidt for the plasmid p1778.16; G. Marschall for excellent technical assistance; and M. Schmidt-Supprian and V. Heissmeyer for helpful discussions. The injection of ES cells into blastocytes was done by M. Hafner and M. Ebel of the Gesellschaft für Biotechnologische Forschung Braunschweig (supported by Nationales Genomforschungsnetz Deutschland).

This work was supported by the Deutsche Forschungsgemeinschaft STR-461/3-2, and Deutsche Krebshilfe. J. Rastelli was supported by the Boehringer Ingelheim Fonds. K. Rajewsky is supported by grants from the National Institutes of Health and the Leukemia and Lymphoma Society, and K. Rajewsky and W. Mueller are supported by the European Union through MUGEN.

The authors declare that they have no conflicting financial interests.

Submitted: 4 February 2008
Accepted: 16 April 2008

REFERENCES

1. van Kooten, C., and J. Banchereau. 2000. CD40-CD40 ligand. *J. Leukoc. Biol.* 67:2–17.
2. DiSanto, J.P., J.Y. Bonnefoy, J.F. Gauchat, A. Fischer, and G. de Saint Basile. 1993. CD40 ligand mutations in x-linked immunodeficiency with hyper-IgM. *Nature.* 361:541–543.
3. Korthauer, U., D. Graf, H.W. Mages, F. Briere, M. Padayachee, S. Malcolm, A.G. Ugazio, L.D. Notarangelo, R.J. Levinsky, and R.A. Kroczek. 1993. Defective expression of T-cell CD40 ligand causes X-linked immunodeficiency with hyper-IgM. *Nature.* 361:539–541.
4. Kawabe, T., T. Naka, K. Yoshida, T. Tanaka, H. Fujiwara, S. Suematsu, N. Yoshida, T. Kishimoto, and H. Kikutani. 1994. The immune responses in CD40-deficient mice: impaired immunoglobulin class switching and germinal center formation. *Immunity.* 1:167–178.
5. Xu, J., T.M. Foy, J.D. Laman, E.A. Elliott, J.J. Dunn, T.J. Waldschmidt, J. Elsemore, R.J. Noelle, and R.A. Flavell. 1994. Mice deficient for the CD40 ligand. *Immunity.* 1:423–431.
6. Grammer, A.C., and P.E. Lipsky. 2000. CD40-mediated regulation of immune responses by TRAF-dependent and TRAF-independent signaling mechanisms. *Adv. Immunol.* 76:61–178.
7. Hostager, B.S., I.M. Catlett, and G.A. Bishop. 2000. Recruitment of CD40 and tumor necrosis factor receptor-associated factors 2 and 3 to membrane microdomains during CD40 signaling. *J. Biol. Chem.* 275:15392–15398.
8. Hanissian, S.H., and R.S. Geha. 1997. Jak3 is associated with CD40 and is critical for CD40 induction of gene expression in B cells. *Immunity.* 6:379–387.
9. Craxton, A., G. Shu, J.D. Graves, J. Saklatvala, E.G. Krebs, and E.A. Clark. 1998. p38 MAPK is required for CD40-induced gene expression and proliferation in B lymphocytes. *J. Immunol.* 161:3225–3236.
10. Li, Y.Y., M. Baccam, S.B. Waters, J.E. Pessin, G.A. Bishop, and G.A. Koretzky. 1996. CD40 ligation results in protein kinase C-independent activation of ERK and JNK in resting murine splenic B cells. *J. Immunol.* 157:1440–1447.
11. Sutherland, C.L., A.W. Heath, S.L. Pelech, P.R. Young, and M.R. Gold. 1996. Differential activation of the ERK, JNK, and p38 mitogen-activated protein kinases by CD40 and the B cell antigen receptor. *J. Immunol.* 157:3381–3390.
12. Berberich, I., G.L. Shu, and E.A. Clark. 1994. Cross-linking CD40 on B cells rapidly activates nuclear factor-kappa B. *J. Immunol.* 153:4357–4366.
13. Coope, H.J., P.G. Atkinson, B. Huhse, M. Belich, J. Janzen, M.J. Holman, G.G. Klaus, L.H. Johnston, and S.C. Ley. 2002. CD40 regulates the processing of NF-kappaB2 p100 to p52. *EMBO J.* 21:5375–5385.
14. Bonizzi, G., and M. Karin. 2004. The two NF-kappaB activation pathways and their role in innate and adaptive immunity. *Trends Immunol.* 25:280–288.
15. Bonizzi, G., M. Bebien, D.C. Otero, K.E. Johnson-Vroom, Y. Cao, D. Vu, A.G. Jegga, B.J. Aronow, G. Ghosh, R.C. Rickert, and M. Karin. 2004. Activation of IKKalpha target genes depends on recognition of specific kappaB binding sites by RelB:p52 dimers. *EMBO J.* 23:4202–4210.
16. Dejardin, E., N.M. Droin, M. Delhase, E. Haas, Y. Cao, C. Makris, Z.W. Li, M. Karin, C.F. Ware, and D.R. Green. 2002. The lymphotoxin-beta receptor induces different patterns of gene expression via two NF-kappaB pathways. *Immunity.* 17:525–535.
17. Derudder, E., E. Dejardin, L.L. Pritchard, D.R. Green, M. Korner, and V. Baud. 2003. RelB/p50 dimers are differentially regulated by tumor necrosis factor-alpha and lymphotoxin-beta receptor activation: critical roles for p100. *J. Biol. Chem.* 278:23278–23284.
18. Eliopoulos, A.G., and L.S. Young. 2004. The role of the CD40 pathway in the pathogenesis and treatment of cancer. *Curr. Opin. Pharmacol.* 4:360–367.
19. Baxendale, A.J., C.W. Dawson, S.E. Stewart, V. Mudaliar, G. Reynolds, J. Gordon, P.G. Murray, L.S. Young, and A.G. Eliopoulos. 2005. Constitutive activation of the CD40 pathway promotes cell transformation and neoplastic growth. *Oncogene.* 24:7913–7923.
20. Challa, A., A.G. Eliopoulos, M.J. Holder, A.S. Burguete, J.D. Pound, A. Chamba, G. Grafton, R.J. Armitage, C.D. Gregory, H. Martinez-Valdez, et al. 2002. Population depletion activates autonomous CD154-dependent survival in biopsylike Burkitt lymphoma cells. *Blood.* 99:3411–3418.
21. Furman, R.R., Z. Asgary, J.O. Mascarenhas, H.C. Liou, and E.J. Schattner. 2000. Modulation of NF-kappa B activity and apoptosis in chronic lymphocytic leukemia B cells. *J. Immunol.* 164:2200–2206.
22. Pham, L.V., A.T. Tamayo, L.C. Yoshimura, P. Lo, N. Terry, P.S. Reid, and R.J. Ford. 2002. A CD40 signalosome anchored in lipid rafts leads to

constitutive activation of NF-kappaB and autonomous cell growth in B cell lymphomas. *Immunity*. 16:37–50.
23. Gires, O., U. Zimber-Strobl, R. Gonnella, M. Ueffing, G. Marschall, R. Zeidler, D. Pich, and W. Hammerschmidt. 1997. Latent membrane protein 1 of Epstein-Barr virus mimics a constitutively active receptor molecule. *EMBO J.* 16:6131–6140.
24. Hatzivassiliou, E., W.E. Miller, N. Raab-Traub, E. Kieff, and G. Mosialos. 1998. A fusion of the EBV latent membrane protein-1 (LMP1) transmembrane domains to the CD40 cytoplasmic domain is similar to LMP1 in constitutive activation of epidermal growth factor receptor expression, nuclear factor-kappa B, and stress-activated protein kinase. *J. Immunol.* 160:1116–1121.
25. Yasui, T., M. Muraoka, Y. Takaoka-Shichijo, I. Ishida, N. Takegahara, J. Uchida, A. Kumanogoh, S. Suematsu, M. Suzuki, and H. Kikutani. 2002. Dissection of B cell differentiation during primary immune responses in mice with altered CD40 signals. *Int. Immunol.* 14:319–329.
26. Kraus, M., M.B. Alimzhanov, N. Rajewsky, and K. Rajewsky. 2004. Survival of resting mature B lymphocytes depends on BCR signaling via the Igalpha/beta heterodimer. *Cell.* 117:787–800.
27. Rickert, R.C., J. Roes, and K. Rajewsky. 1997. B lymphocyte-specific, Cre-mediated mutagenesis in mice. *Nucleic Acids Res.* 25:1317–1318.
28. Bennett, B.L., D.T. Sasaki, B.W. Murray, E.C. O'Leary, S.T. Sakata, W. Xu, J.C. Leisten, A. Motiwala, S. Pierce, Y. Satoh, et al. 2001. SP600125, an anthrapyrazolone inhibitor of Jun N-terminal kinase. *Proc. Natl. Acad. Sci. USA.* 98:13681–13686.
29. Favata, M.F., K.Y. Horiuchi, E.J. Manos, A.J. Daulerio, D.A. Stradley, W.S. Feeser, D.E. Van Dyk, W.J. Pitts, R.A. Earl, F. Hobbs, et al. 1998. Identification of a novel inhibitor of mitogen-activated protein kinase kinase. *J. Biol. Chem.* 273:18623–18632.
30. Panagopoulos, D., P. Victoratos, M. Alexiou, G. Kollias, and G. Mosialos. 2004. Comparative analysis of signal transduction by CD40 and the Epstein-Barr virus oncoprotein LMP1 in vivo. *J. Virol.* 78:13253–13261.
31. Bangs, S.C., A.J. McMichael, and X.N. Xu. 2006. Bystander T cell activation–implications for HIV infection and other diseases. *Trends Immunol.* 27:518–524.
32. Ehl, S., J. Hombach, P. Aichele, H. Hengartner, and R.M. Zinkernagel. 1997. Bystander activation of cytotoxic T cells: studies on the mechanism and evaluation of in vivo significance in a transgenic mouse model. *J. Exp. Med.* 185:1241–1251.
33. Koschella, M., D. Voehringer, and H. Pircher. 2004. CD40 ligation in vivo induces bystander proliferation of memory phenotype CD8 T cells. *J. Immunol.* 172:4804–4811.
34. Taraban, V.Y., T.F. Rowley, and A. Al-Shamkhani. 2004. Cutting edge: a critical role for CD70 in CD8 T cell priming by CD40-licensed APCs. *J. Immunol.* 173:6542–6546.
35. Morse, H.C. III, M.R. Anver, T.N. Fredrickson, D.C. Haines, A.W. Harris, N.L. Harris, E.S. Jaffe, S.C. Kogan, I.C. MacLennan, P.K. Pattengale, and J.M. Ward. 2002. Bethesda proposals for classification of lymphoid neoplasms in mice. *Blood.* 100:246–258.
36. Vonderheide, R.H., J.P. Dutcher, J.E. Anderson, S.G. Eckhardt, K.F. Stephans, B. Razvillas, S. Garl, M.D. Butine, V.P. Perry, R.J. Armitage, et al. 2001. Phase I study of recombinant human CD40 ligand in cancer patients. *J. Clin. Oncol.* 19:3280–3287.
37. Fiumara, P., and A. Younes. 2001. CD40 ligand (CD154) and tumour necrosis factor-related apoptosis inducing ligand (Apo-2L) in haematological malignancies. *Br. J. Haematol.* 113:265–274.
38. Basak, S., H. Kim, J.D. Kearns, V. Tergaonkar, E. O'Dea, S.L. Werner, C.A. Benedict, C.F. Ware, G. Ghosh, I.M. Verma, and A. Hoffmann. 2007. A fourth IkappaB protein within the NF-kappaB signaling module. *Cell.* 128:369–381.
39. Hoffmann, A., and D. Baltimore. 2006. Circuitry of nuclear factor kappaB signaling. *Immunol. Rev.* 210:171–186.
40. Annunziata, C.M., R.E. Davis, Y. Demchenko, W. Bellamy, A. Gabrea, F. Zhan, G. Lenz, I. Hanamura, G. Wright, W. Xiao, et al. 2007. Frequent engagement of the classical and alternative NF-kappaB pathways by diverse genetic abnormalities in multiple myeloma. *Cancer Cell.* 12:115–130.
41. Keats, J.J., R. Fonseca, M. Chesi, R. Schop, A. Baker, W.J. Chng, S. Van Wier, R. Tiedemann, C.X. Shi, M. Sebag, et al. 2007. Promiscuous mutations activate the noncanonical NF-kappaB pathway in multiple myeloma. *Cancer Cell.* 12:131–144.
42. Horie, R., T. Watanabe, Y. Morishita, K. Ito, T. Ishida, Y. Kanegae, I. Saito, M. Higashihara, S. Mori, M.E. Kadin, and T. Watanabe. 2002. Ligand-independent signaling by overexpressed CD30 drives NF-kappaB activation in Hodgkin-Reed-Sternberg cells. *Oncogene.* 21:2493–2503.
43. McCubrey, J.A., L.S. Steelman, W.H. Chappell, S.L. Abrams, E.W. Wong, F. Chang, B. Lehmann, D.M. Terrian, M. Milella, A. Tafuri, et al. 2007. Roles of the Raf/MEK/ERK pathway in cell growth, malignant transformation and drug resistance. *Biochim. Biophys. Acta.* 1773:1263–1284.
44. Zheng, B., P. Fiumara, Y.V. Li, G. Georgakis, V. Snell, M. Younes, J.N. Vauthey, A. Carbone, and A. Younes. 2003. MEK/ERK pathway is aberrantly active in Hodgkin disease: a signaling pathway shared by CD30, CD40, and RANK that regulates cell proliferation and survival. *Blood.* 102:1019–1027.
45. Soriano, P. 1999. Generalized lacZ expression with the ROSA26 Cre reporter strain. *Nat. Genet.* 21:70–71.
46. Lakso, M., B. Sauer, B. Mosinger Jr., E.J. Lee, R.W. Manning, S.H. Yu, K.L. Mulder, and H. Westphal. 1992. Targeted oncogene activation by site-specific recombination in transgenic mice. *Proc. Natl. Acad. Sci. USA.* 89:6232–6236.
47. Ruland, J., G.S. Duncan, A. Elia, I. del Barco Barrantes, L. Nguyen, S. Plyte, D.G. Millar, D. Bouchard, A. Wakeham, P.S. Ohashi, and T.W. Mak. 2001. Bcl10 is a positive regulator of antigen receptor-induced activation of NF-kappaB and neural tube closure. *Cell.* 104:33–42.
48. Ruland, J., G.S. Duncan, A. Wakeham, and T.W. Mak. 2003. Differential requirement for Malt1 in T and B cell antigen receptor signaling. *Immunity.* 19:749–758.